

Remarkably low turn-on field emission in undoped, nitrogen-doped, and boron-doped graphene

U. A. Palnitkar,¹ Ranjit V. Kashid,² Mahendra A. More,² Dilip S. Joag,² L. S. Panchakarla,¹ and C. N. R. Rao^{1,a)}

¹International Centre for Materials Science, Chemistry and Physics of Materials Unit, CSIR Centre of Excellence in Chemistry, Jawaharlal Nehru Centre for Advanced Scientific Research, Jakkur P.O., Bangalore 560064, India

²Department of Physics, Center for Advanced Studies in Material Science and Condensed Matter Physics, University of Pune, Pune 411007, India

(Received 29 May 2010; accepted 18 June 2010; published online 9 August 2010)

Field emission studies have been carried out on undoped as well as N- and B-doped graphene samples prepared by arc-discharge method in a hydrogen atmosphere. These graphene samples exhibit very low turn-on fields. N-doped graphene shows the lowest turn-on field of 0.6 V/ μm , corresponding to emission current density of 10 $\mu\text{A}/\text{cm}^2$. These characteristics are superior to the other types of nanomaterials reported in the literature. Furthermore, emission currents are stable over the period of more than 3 h for the graphene samples. The observed emission behavior has been explained on the basis of nanometric features of graphene and resonance tunneling phenomenon.

© 2010 American Institute of Physics. [doi:10.1063/1.3464168]

Electron sources are becoming increasingly important for use in both research and technological applications. While conventional thermoelectronic emitters seem to be declining in importance, cold electron emitters using field emission are showing great potential for several applications. Among the numerous nanomaterials, electron field emission cathodes based on carbon nanocrystalline materials are being extensively investigated for high current density applications.¹⁻⁴ Thus, carbon nanotubes and nanofibers have been frequently used for fabricating field emission cathodes because of their high aspect ratios as well as unique mechanical and electronic properties. These materials exhibit low turn-on voltages and large emission current densities.^{5,6} Most recently, graphene, the two-dimensional nanocarbon has attracted great attention because of its exceptional properties.^{7,8} In addition to possible applications in ultrahigh-speed nanoelectronics,⁹ graphene promises to be useful in chemical and biosensor.^{10,11} There have been attempts to investigate field emission properties of graphene films recently.¹²⁻¹⁴ A spin-coated graphene film is reported to exhibit a threshold field (for a current of $10^{-8}\text{A}/\text{cm}^2$) of 4 V/ μm with a field enhancement factor, β , of 1200.¹² A few-layer graphene film synthesized by chemical vapor deposition exhibits a favorable turn-on field but decays after five cycles, the turn-on field shifting to 3 V/ μm and β decreasing to 3000.¹³ Use of electrophoretic deposition appears to lower the turn-on voltage.¹⁴ Besides geometrical factors and spatial distribution, tailoring the work function provides another means to improve the electron field emission. Theoretical studies have shown that substitutional doping can modulate the band structure of graphene.^{15,16}

We have carried out a careful investigation of the field emission properties of undoped, as well as boron- and nitrogen-doped graphenes. For this purpose, we have prepared these graphene samples by carrying out arc discharge

of graphite with appropriate doping methodologies, since arc discharge is expected to yield graphene samples with higher conductivity.¹⁷ We carried out arc discharge in the presence of hydrogen to obtain 2–3 layers of graphene (HG) [Fig. 1(a)]. To prepare boron-doped graphene (BG), we carried out arc discharge in the presence of $\text{H}_2 + \text{B}_2\text{H}_6$. We prepared nitrogen-doped graphene (NG) by carrying out the arc discharge in the presence of $\text{H}_2 +$ pyridine.^{18,19} All the above mentioned graphene samples were characterized by variety of physical characterization techniques. Based on the XPS measurements, BG and NG were found to contain 1.2 at. % of boron and 0.6 at. % of nitrogen, respectively. Electron energy loss spectroscopy measurements performed in an electron microscope indicated that the contents of boron and nitrogen to be comparable to those obtained from XPS.

Electrophoretic deposition was employed for depositing vertically oriented graphene sheets²⁰ for the electron field emission measurements. Figure 1(b) shows field emission scanning electron microscope images of HG, BG, and NG samples obtained after deposition on Si substrate. The films are randomly oriented with high graphene density and uni-

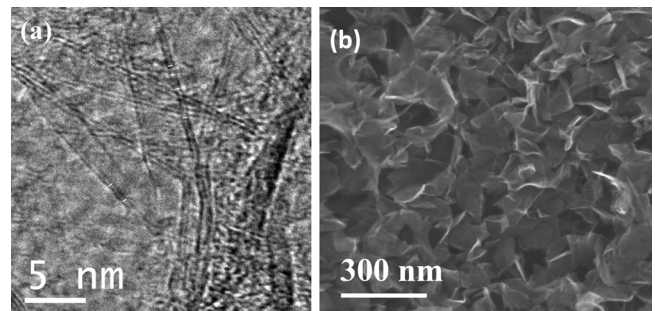


FIG. 1. (a) High magnification transmission electron microscopy image of undoped graphene (HG) showing the presence of 2–3 layers. (b) field-emission scanning electron microscopy image of graphene films obtained after deposition on Si substrate undoped graphene (HG).

^{a)}Author to whom correspondence should be addressed. Electronic mail: cnrrao@jncasr.ac.in. FAX: (+91) 80-22082760.

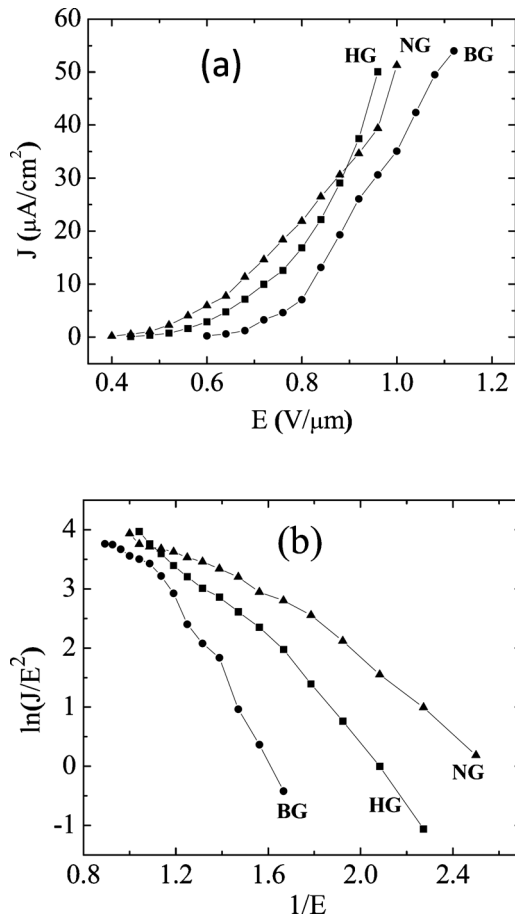


FIG. 2. (a) Current density (j) of undoped (HG), boron-doped (BG), and nitrogen-doped (NG) graphenes as a function of electric field. (b) FN plot of HG, BG, and NG graphenes.

form morphology. The sharp edges present function as emission sites and enhance the field emission.

The graphene samples deposited on Si substrate were loaded independently on a copper stub by using conducting vacuum compatible silver paste in such a manner as to be parallel to the phosphor coated conducting glass anode screen. The distance between the cathode and anode was manipulated by using a linear mechanical drive. After mounting the sample inside the ultrahigh vacuum chamber, the chamber was baked at 250°C for 10 h to achieve a base pressure of 1×10^{-8} mbar. Field emission current density–electric field (J - E) and the emission current–time stability (I - t) characteristics were measured at the same base pressure using a Keithley 6514 picoammeter and a Spellman high voltage dc power supply at room temperature. The interelectrode separation was kept at 1 mm throughout the experiments.

Figure 2(a) shows the variation in J - E characteristics of the HG, BG, and NG samples. The turn-on electric field (defined as the field required to draw the current density of $10 \mu\text{A}/\text{cm}^2$) is 0.7, 0.8, and 0.6 $\text{V}/\mu\text{m}$ for HG, BG, and NG, respectively. As the applied voltage was increased further, the emission current density of $\sim 50 \mu\text{A}/\text{cm}^2$ was drawn at an applied field of 0.95, 1.08, and 0.99 $\text{V}/\mu\text{m}$ for HG, BG, and NG, respectively. These values are found to be significantly lower than the best values reported for graphene samples,^{20–22} subnanometer graphite sheets,²³ undoped and doped carbon nanotubes,^{24–26} and other semiconducting na-

nomaterials such as CdS aligned nanowires,²⁷ tungsten oxide nanowires²⁸ and ZnO needles.²⁹ The smaller turn-on electric field observed by us is thus noteworthy and probably results from the unique characteristics of the graphene prepared by arc discharge in hydrogen.

The Fowler–Nordheim (FN) model of field emission originating from the study of flat metallic surfaces at 0 K is widely used in carbon based electron emitters.³⁰ We have used Eq. (1) to calculate the field enhancement factor, β .

$$J = A(\beta^2 E^2 / \Phi) \exp(-B\Phi^{1.5} / \beta E). \quad (1)$$

Here, J is the emission current density, $A(1.54 \times 10^{-6} \text{ A eV}/\text{V}^2)$ and $B(6.8 \times 10^9 \text{ eV}^{-3/2} \text{ V}/\text{m})$ are constant, Φ is the work function and is assumed to be 5 eV same as that for graphite. The FN theory is valid only for metallic emitters. In the case of semiconducting emitters, effects such as field penetration and band bending will have to be considered but there is no unified equation or theory which accounts for all these parameters for both semiconducting and metallic emitters. Hence, one uses the FN equation for the analysis of field emission data. In the present study, the FN plot is found to be nonlinear and such FN plots have been reported for many semiconducting nanomaterials.^{31,32} The nonlinearity in the FN plot can be resolved into two linear sections with distinct slopes in the high-field and low-field regions [see Fig. 2(b)]. The field enhancement factors (β) are calculated from the slope of the low-field and the high-field regions of the FN plot, using the following equation,

$$\beta = (6.8 \times 10^3 \times \Phi^{3/2}) / \text{slope} \quad (2)$$

are found to be 15740, 11879, 25849 for the low-field region and 24058, 12067, 49690 for the high-field region of HG, BG, NG, respectively. These calculated values of β may be overestimates due to the limitation of the FN equation.

The small turn-on field is associated with the edges of vertically oriented graphene sheets. Furthermore, N-doped graphene shows the lowest turn-on field, relative to undoped graphene. One of the reasons probably is the up-shift of the Fermi level of graphene due to N-doping.¹⁸ The turn on voltage depends upon the local field through β , the charge carrier density, and the type of doping (donor or acceptor). In addition to these parameters, resonance tunneling may also play a role.³³ Our field emission patterns consist of random spots, unlike emission from single graphene sheet²⁰ suggestive of resonance tunneling. Field emission includes transfer of electrons from the electrode to the field emitting material, and subsequently transit of electrons into the material, finally going to the vacuum. For a given material, the first and the last steps are important factors.^{13,22,34,35}

Stability of the field emission current is an important requirement for practical applications of cold cathodes. We have measured the stability of HG, BG, and NG at a current value of $1 \mu\text{A}$ over a duration of more than 3 h by using a controlled data acquisition system, acquiring the emission current data with a sampling time of 10 s. Figure 3 shows the current–time plots measured at a base pressure of 1×10^{-8} mbar. Ignoring short-term fluctuations due to adsorption and desorption of residual gas molecules and diffusion of adsorbed species on the emitter surface, the I - t plots are nearly identical after repetitive measurements with no degradation in the emission current during long term operation (Fig. 3). The field emission patterns shown as insets in

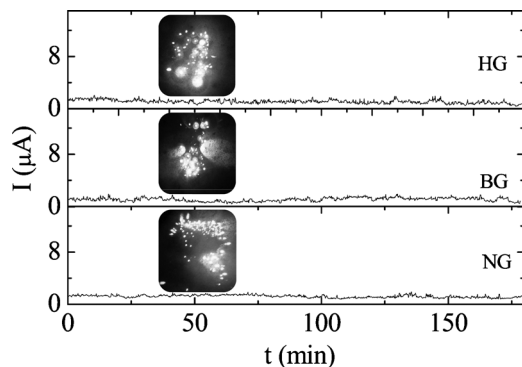


FIG. 3. Current stability of undoped (HG), boron-doped (BG), and nitrogen-doped (NG) graphenes (Inset field emission pattern corresponding to HG, BG, and NG).

Fig. 3 reveal tiny spots and the number of emission spots does not change during I-t measurements. The postfield-emission surface morphology shows no deterioration of the emitter surface indicating its mechanical robustness against ion bombardment and field-induced stress.

In conclusion, we have employed electrophoresis to fabricate undoped and doped graphene films synthesized by arc-discharge in hydrogen and studied their field emission properties. These high-density graphene films exhibit better field emission properties than other nanostructures, with a turn-on electric field of ~ 0.7 V/ μm . The excellent field emission properties of graphene appear to arise from the intrinsic properties such as electrical conductivity, morphological features, and resonance tunneling.

L.S.P. would like to acknowledge CSIR for senior research fellowship. R.V.K. thanks to UGC for financial support. D.S.J. would like to thank to CNQS. The field emission work has been carried out as a part of the CNQS (UPE-UGC program) activity.

¹N. de Jonge, Y. Lamy, K. Schoots, and T. Oosterkamp, *Nature (London)* **420**, 393 (2002).

²R. H. Baughman, A. A. Zakhidov, and W. A. Heer, *Science* **297**, 787 (2002).

³J. Kong, N. R. Franklin, C. W. Zhou, M. G. Chapline, S. Peng, and K. J. Cho, *Science* **287**, 622 (2000).

⁴P. G. Collins, K. Bradley, M. Ishigami, and A. Zett, *Science* **287**, 1801 (2000).

⁵W. A. de Heer, A. Chatelian, and D. Ugarte, *Science* **270**, 1179 (1995).

⁶S. I. Cha, K. T. Kim, S. N. Arshad, C. B. Mo, K. H. Lee, and S. H. Hong, *Adv. Mater.* **18**, 553 (2006).

⁷A. K. Geim, *Science* **324**, 1530 (2009).

⁸C. N. R. Rao, A. K. Sood, K. S. Subrahmanyam, and A. Govindaraj, *Angew. Chem.* **48**, 7752 (2009).

⁹Y. M. Lin, K. A. Jenkins, A. V. Garcia, J. P. Small, and P. Avouris, *Nano Lett.* **9**, 422 (2009).

¹⁰F. Schedin, A. K. Geim, S. V. Morozov, E. W. Hill, P. Blake, and M. I. Katsnelson, *Nature Mater.* **6**, 652 (2007).

¹¹N. M. Mohanty and V. Berry, *Nano Lett.* **8**, 4469 (2008).

¹²G. Eda, H. E. Unalan, N. Rupensinghe, G. A. J. Amartunga, and M. Chhowalla, *Appl. Phys. Lett.* **93**, 233502 (2008).

¹³A. Malesevic, R. Kemps, A. Vanhulsel, M. P. Chowdhary, and A. Volodin, *J. Appl. Phys.* **104**, 084301 (2008).

¹⁴S. M. Jung, J. Hahn, H. Y. Jung, and J. S. Suh, *Nano Lett.* **6**, 1569 (2006).

¹⁵F. Cervantes-Sodi, G. Csanyi, S. Piscanec, and A. Ferrari, *Phys. Rev. B* **77**, 165427 (2008).

¹⁶M. Calandra and F. Mauri, *Phys. Rev. B* **76**, 161406 (2007).

¹⁷D. J. Late, A. Ghosh, K. S. Subrahmanyam, L. S. Panchakarla, S. B. Krupanidhi, and C. N. R. Rao, *Solid State Commun.* **150**, 734 (2010).

¹⁸L. S. Panchakarla, K. S. Subrahmanyam, S. K. Saha, A. Govindaraj, H. R. Krishnamurthy, U. V. Waghmare, and C. N. R. Rao, *Adv. Mater.* **21**, 4726 (2009).

¹⁹K. S. Subrahmanyam, L. S. Panchakarla, A. Govindaraj, and C. N. R. Rao, *J. Phys. Chem. C* **113**, 4257 (2009).

²⁰Z. S. Wu, S. Pei, W. Ren, D. Tang, L. Gao, B. Liu, F. Li, C. Liu, and H. M. Cheng, *Adv. Mater.* **21**, 1756 (2009).

²¹J. L. Qi, X. Wang, W. T. Zheng, H. W. Tian, C. Q. Hu, and Y. S. Peng, *J. Phys. D: Appl. Phys.* **43**, 055302 (2010).

²²M. Qian, T. Feng, H. Ding, L. Lin, H. Li, and Y. C. Z. Sun, *Nanotechnology* **20**, 425702 (2009).

²³J. J. Wang, M. Y. Zhu, R. A. Outlaw, X. Zhao, D. M. Manos, B. C. Holloway, and V. P. Mammana, *Appl. Phys. Lett.* **85**, 1265 (2004).

²⁴J. M. Bonard, J. P. Salvetat, and T. Stockli, *Appl. Phys. Lett.* **73**, 918 (1998).

²⁵J. C. Charlier, M. Terrones, M. Baxendale, V. Meunier, T. Zacharia, N. L. Rupensinghe, W. K. Hsu, N. Grobert, H. Terrones, and G. A. J. Amartunga, *Nano Lett.* **2**, 1191 (2002).

²⁶S. K. Srivastava, V. D. Vankar, D. V. Sridhar, and V. Kumar, *Thin Solid Films* **515**, 1851 (2006).

²⁷A. Datta, P. G. Chavan, F. J. Sheini, M. A. More, D. S. Joag, and A. Patra, *Cryst. Growth Des.* **9**, 4157 (2009).

²⁸D. J. Late, R. V. Kashid, C. S. Rout, M. A. More, and D. S. Joag, *Appl. Phys. A: Mater. Sci. Process.* **98**, 751 (2010).

²⁹C. J. Park, D. K. Choi, J. Yoo, G. C. Yi, and C. J. Lee, *Appl. Phys. Lett.* **90**, 083107 (2007).

³⁰R. H. Fowler and L. W. Nordheim, *Proc. R. Soc. London, Ser. A* **119**, 173 (1928).

³¹N. S. Ramgir, D. J. Late, A. B. Bhise, I. S. Mulla, M. A. More, D. S. Joag, and V. K. Pillai, *Nanotechnology* **17**, 2730 (2006).

³²N. S. Ramgir, D. J. Late, A. B. Bhise, M. A. More, I. S. Mulla, D. S. Joag, and K. Vijayamohanam, *J. Phys. Chem. B* **110**, 18236 (2006).

³³J. W. Gadzuk, *Phys. Rev. B* **47**, 12832 (1993).

³⁴T. Connolly, R. C. Smith, Y. Hernandez, Y. G. Ko, J. N. Coleman, and J. D. Carey, *Small* **5**, 826 (2009).

³⁵R. C. Smith, J. D. Carey, R. J. Murphy, W. J. Blau, J. N. Coleman, and S. R. P. Silva, *Appl. Phys. Lett.* **87**, 263105 (2005).